J. Cell. Mol. Med. Vol 12, No 2, 2008 pp. 622-638

Oval cell proliferation in p16^{INK4a} expressing mouse liver is triggered by chronic growth stimuli

Elke Ueberham [a], Ricco Lindner [b], Manja Kamprad [c], Rico Hiemann [c], Nadja Hilger [c], Barbara Woithe [a], Doris Mahn [a], Michael Cross [d], Ulrich Sack [c], Rolf Gebhardt [a], Thomas Arendt [b], Uwe Ueberham [b, *]

[a] Institute of Biochemistry, University of Leipzig, Medical Faculty, Leipzig, Germany
[b] Paul-Flechsig-Institute of Brain Research, Department of Neuroanatomy, University of Leipzig, Medical Faculty, Leipzig, Germany
[c] Institute of Clinical Immunology and Transfusion Medicine, Medical Faculty, Leipzig, Germany
[d] Department of Haematology / Oncology, Medical Faculty, University of Leipzig, Leipzig, Germany

Received: July 20, 2007; Accepted: October 18, 2007

Abstract

Terminal differentiation requires molecules also involved in aging such as the cell cycle inhibitor p16^{INK4a}. Like other organs, the adult liver represents a quiescent organ with terminal differentiated cells, hepatocytes and cholangiocytes. These cells retain the ability to proliferate in response to liver injury or reduction of liver mass. However, under conditions which prevent mitotic activation of hepatocytes, regeneration can occur instead from facultative hepatic stem cells. For therapeutic application a non-toxic activation of this stem cell compartment is required. We have established transgenic mice with conditional overexpression of the cell cycle inhibitor p16^{INK4a} in hepatocytes and have provoked and examined oval cell activation in adult liver in response to a range of proliferative stimuli. We could show that the liver specific expression of p16^{INK4a} leads to a faster differentiation of hepatocytes and an activation of oval cells already in postnatal mice without negative consequences on liver function.

Keywords: p16^{INK4a} • hepatic stem cell • oval cell • nodularin • starvation • tet-system

Introduction

P16^{INK4a} is an inhibitor of cell cycle progression that binds specifically to cyclin-dependent kinases (CDKs) 4 and 6, preventing the formation of the CDK/cyclin D1 complexes which normally phosphorylate retinoblastoma protein (RB) to allow progression through the G1/S checkpoint [1]. There is no evidence of an essential role for p16^{INK4a} in development, with expression being undetectable in mouse embryos [2] and development apparently normal in knock out mice [3, 4]. However, expression increases with age in both mice and humans [5], consistent with a role in terminal differentiation and senescence. Indeed, p16^{INK4a} contributes to the impaired cellular regeneration of an aging organism and acts as a marker in this process [6].

Consistent with a decisive role in tissue homeostasis, alterations in expression of p16^{INK4a} have been implicated in a variety of disease processes including cardiomyopathy [7], Morbus Alzheimer [8, 9] and a

Correspondence to: Uwe UEBERHAM,
Paul-Flechsig-Institute of Brain Research, Department of Neuroanatomy, University of Leipzig, Medical Faculty,
04105 Leipzig, Germany.
Tel.: +49 (0) 34 19 72 57 37
Fax: +49 (0) 34 19 72 57 29
E-mail: Uwe.Ueberham@medizin.uni-leipzig.de

doi: 10.1111/j.1582-4934.2007.00178.x

wide range of cancers [10, 11]. Here, classic tumour suppressor function has been confirmed by the increased susceptibility of the knock-out mice to a range of cancers [3, 4]. Furthermore, the specific involvement of $p16^{INK4a}$ in liver cancer is indicated both by frequent deletion of the locus in hepatocarcinoma [12, 13], and by an association between $p16^{INK4a}$ expression level and hepatocarcinoma susceptibility in rats [14, 15].

Adult liver is a quiescent organ incorporating highly differentiated epithelial cells (hepatocytes and cholangiocytes) and mesenchymal cells (Kupffer cells, endothelial cells and hepatic stellate cells). The hepatocytes account for approximately 70% of liver cells and are arrested in the G0 phase of cell cycle [16], but retain the unusual ability to re-enter cycle in order to regenerate large amounts of tissue in response to liver injury [17]. Under conditions which prevent the mitotic activation of hepatocytes, regeneration can occur instead from a distinct population of hepatic stem cells (oval cells) which reside in the canal of hering, a well-defined zone between hepatocytes and cholangiocytes of the biliary epithelium [18, 19]. Oval cells are considered to be bi-potential epithelial stem cells capable of regenerating both hepatocytes and cholangiocytes (for review see [20]).

While the potential use of somatic stem cells for therapeutic applications has raised interest in mechanisms of liver regeneration in recent years, models of oval cell recruitment to date have all involved chemically induced injury which compromises therapeutic potential [21]. In order to generate a non-cytotoxic model of oval cell recruitment, we have established transgenic mice with conditional overexpression of the cell cycle inhibitor $p16^{INK4a}$ in hepatocytes, thereby permitting the investigation of $p16^{INK4a}$ overexpression in liver in all phases of development. Using these mice, we have examined oval cell activation in adult liver in response to a range of proliferative stimuli.

Materials and methods

Cloning of human $p16^{INK4a}$ cDNA and generation of transgenic mice

For cloning $p16^{INK4a}$ cDNA human fibroblast RNA was isolated, reverse transcribed using random pdN_6-primers and Superscript II RT (Gibco, Eggenstein, Germany), and the obtained cDNA was amplified using the following specific primer pairs containing MluI and HindIII sites allowing subcloning into pBI vector (p16-Mlu-F: ctcacgcgtagcgggagcagcatggagccggcg; p16-Hind-R: atcaagcttgctctggttctttcaatcggggat). Transgenic mice with inducible hepatocyte-specific expression of $p16^{INK4a}$ were generated using the heterologous tTA system [22] as illustrated in Figure 1. Briefly, individuals of transgenic line $p_{tet}p16^{INK4a}$ (C57Bl/6-DBA background) carrying the bi-directional transcription unit for luciferase and $p16^{INK4a}$ were interbred with individuals of the transactivator line TA^{LAP-2} (C57Bl/6-NMRI background) [23]. Double transgenic mice $p_{tet}p16^{INK4a}/TA^{LAP-2}$ were interbred with C57Bl/6-Tg(ACT-EGFP)1Osb/J mice expressing the green fluorescence protein [24] to obtain triple transgenic mice $p_{tet}p16^{INK4a}/TA^{LAP-2}$/EGFP for isolating labelled cells.

Animal treatment

Animals were housed under a constant day-night cycle of 12:12 hours and fed a standard chow diet (Altromin 1324, Altromin Gesellschaft für Tierernährung, Lage, Germany), with access to water/doxycycline hydrochloride solution *ad libitum* under all conditions. Animal experiments were carried out in accordance with the European Council Directive of November 24, 1986 (86/609/EEC) and were approved by the local authorities.

Doxycycline hydrochlorid (Dox; Sigma, Deisenhofen, Germany) was dissolved to 50 µg/ml in water and given in brown bottles, which were exchanged twice a week, to prevent transcription. Expression of transgenic proteins was induced by substituting plain water for Dox. $P16^{INK4a}$ expressing mice and controls were treated with nodularin (25 µg/kg body weight, MP Biomedicals, Aurora, OH, USA) thrice weekly by i.p. injections over 4 to 16 weeks and killed 1 day (NDLN) or 4 weeks ($NDLN^{+}$) after this treatment.

Starvation and re-feeding (interval feeding) was performed as previously described [25]. Briefly, animals were given no food over a period of 48 hrs, but water/Dox *ad libitum* and then re-feeded 24 hrs. This procedure was repeated ten times.

Partial hepatectomy (PH) was performed according to the method of Greene and Puder (2003) [26] with slight modifications under ketamine/xylazine anaesthesia. Briefly, food was withdrawn at 6 a.m. and surgery was done between 1 to 3 p.m. Total body weight and weight of removed liver lobes was recorded and the removed portion was calculated using the formula (removed liver pieces in g/0.045*body weight)*100%, in which 0.045 is the mean index of liver weight to body weight of 12-week-old male double transgenic mice of the $p_{tet}p16^{INK4a}/TA^{LAP-2}$ line.

Fifty to 60% of liver was resected and after closing the abdomen 5 ml sterile saline was given subcutaneously on the back. Animals were monitored post-operatively and methamizol-sodium (5 mg/mouse/day) was given in drinking water for analgesia.

Isolation of liver cells, flow cytometric analysis and cell culture

Hepatocytes and oval cells were isolated using an *in vitro* perfusion technique [27].

For preparation of hepatocytes liver was perfused with calcium-free buffered saline and subsequently with collagenase (1 mg/ml, 240 U/mg, Biochrom AG, Berlin, Germany). Cell suspension was centrifuged thrice at 70 x g, 5 min. Hepatocytes were counted and 200,000 cells were re-suspended in 100 µl wash buffer (PBS, 5% FCS) and incubated with an rat anti-mouse CD45 antibody (FITC) (1:40, Serotec, Oxford, UK) 30 min at room temperature to identify contaminating cells. After washing 500 µl ice-cold ethanol (–20°C) were added slowly with continuous mixing avoiding agglutination. Hepatocytes were kept 10 min on ice, washed twice with 1 ml PBS/5% FCS and incubated 1 hr with RNAse A solution (1mg/ml in PBS) at 37°C. Suspension was filled up to 200 µl with PBS/5% FCS and 20 µl propidium iodide (1 mg/ml) were added. This hepatocyte suspension was measured on a flow cytometer (FACScan, Becton Dickinson, Mountain View, CA, USA) for determining the ploidy grade.

Oval cells were isolated by perfusing liver consecutively with calcium-free buffered saline, pronase (1 mg/ml) and collagenase (1 mg/ml) for 10 min each. Cell suspension was centrifuged twice at 70 x *g* disposing the hepatocytes and twice at 250 x *g* for washing and collecting non-parenchymal cells. Cell suspension was than loaded on a discontinuous Percoll gradient to separate oval cells from both other non-parenchymal cells and cellular debris. After density gradient centrifugation (1 hr at 500 x *g*) cells banded at a density of 1.07 were harvested and washed three times in William's E medium. Cells were seeded in either 90-mm culture dishes or flaks and were cultured in William's E medium supplemented with 10% FCS, 2 mM glutamine as clones after trypsination in clonal rings or as whole cell preparation after differential trypsination.

Microarray

Murine Genome Arrays U74Av2 (Affymetrix®) were applied. Following Affymetrix recommendation first strand synthesis was performed using Superscript II RT (Gibco) and second strand synthesis using T4 polymerase. Phenol/chloroform extracted cDNA was used as template for synthesis of biotinylated anti-sense cRNA with the Enzo Bioarray High Yield RNA Transcript Labeling kit. Hybridization and washing were performed according Affymetrix recommendation with fluidics station (Affymetrix®) and scanned with a laser scanner (Agilent Tech®) at 570 nm.

RNA isolation and real time RT-PCR

Total RNA was isolated using the PeqGOLD RNA Pure isolation system (Peqlab, Erlangen, Germany). A cleanup of total RNA was performed using the Qiagen RNeasy Total RNA isolation kit (Qiagen, Hilden, Germany). Quality of RNA was assessed by electrophoresis in denaturing formaldehyde agarose gels and purity was estimated by ratio A260/A280 nm spectrophotometrically. Concentration was adjusted to 1 mg/ml and RNA was stored at –80°C until use. RT-PCR for real time quantification was performed using cyclin D1 specific primers as previously described [28].

Luciferase assay

Liver tissue (100 mg) was homogenized and incubated 5 min in luciferase lysis buffer (500 µl, 77 mM K_2HPO_4, 23 mM KH_2PO_4, 0.2% Triton, 1 mM DTT). The homogenate was centrifuged 5 min in a microcentrifuge. Ten microlitres of the supernatant was applied for measurement of luciferase activity using Luciferase-Assay Reagenz (Promega, Heidelberg, Germany).

Western analysis

Liver tissue was homogenized in cold extraction buffer (10 mM Tris, 150 mM NaCl, 1% NP-40, 0.1% SDS, 1 mM EDTA, 1 x protease inhibitor cocktail (Roche, Mannheim, Germany)) at 4°C followed by sonication. Lysates were cleared by centrifugation and protein was quantified using standard Bradford assay. Samples were separated by SDS-PAGE and transferred to PVDF membranes (GE Healthcare, Freiburg, Germany). Membranes were washed in Tris-buffered saline (TBS)/Tween and blocked in 5% non-fat dry milk and subsequently incubated with the primary antibody listed in Table 1 together with an anti-actin antibody as loading control following the multiplex detection protocol of ECL Plex Western blotting system (GE Healthcare, Freiburg, Germany). Secondary CyDye labelled antibodies were diluted 1:2500 and detected after wash steps by scanning the membrane using a fluorescent laser scanner (Typhoon 9410 Imager, GE Healthcare). Western blots detecting the mouse p16 expression levels were performed using the Chemiluminescence detection system (Pierce, Bonn, Germany).

Table 1: Antibodies used in western analysis (WB) and immunohistochemistry (IHC)

Antibody	Dilution	Supplier
Human-p16^{INK4a} (C20)	1:2000 (WB), 1:300- to 1:1000 (IHC)	Santa Cruz Biotechnology (Heidelberg, Germany)
Human-p16^{INK4a} (N-20)	1:2000 (WB), 1:300- to 1:1000 (IHC)	Santa Cruz Biotechnology
Mouse-p16^{INK4a} (M-156)	1:2000 (WB), 1:300 (IHC)	Santa Cruz Biotechnology
Human- p16^{INK4a} (clone G175-405)	1:5000 (WB)	Pharmingen (BD Biosciences Pharmingen, Erembodegem, Belgium)
p27^{Kip1}	1:1000 (WB)	Neo Markers (Lab Vision Corp., Fremont, CA, USA)
CDK4	1:1000 (WB)	Santa Cruz Biotechnology
CDK6	1:1000 (WB)	Santa Cruz Biotechnology
Cyclin D1	1:1000 (WB)	Stressgen (Ann Arbor, MI, USA)
Cyclin E	1:1000 (WB)	Santa Cruz Biotechnology
PCNA	1:1000 (WB), 1:50 (IHC)	Santa Cruz Biotechnology
glutamine synthetase	1:1000 (IHC)	BD Transduction Lab
carbamoyl phosphatase	1:2000 (IHC)	W. Lamers (Amsterdam, Netherlands)
Cytochrome-P450 IIE1	1:1000 (IHC)	Stressgene
A6	1:100 (IHC)	N. Engelhardt (Moscow, Russia)
E-Cadherin	1:1000 (IHC)	BD Transduction Lab (Heidelberg, Germany)
β-actin	1:2500 (WB)	Abcam (Cambridge, UK)
β-actin	1:10,000 (WB)	Sigma (Schnelldorf, Germany)

Histology and immunohistochemistry

Liver samples were either quick-frozen in liquid nitrogen and stored at –80°C or fixed in 4% paraformaldehyde and routinely embedded in paraffin. Frozen liver samples were used for A6-immunohistochemistry. Liver tissue was cut in 5-μm -thick sections and mounted on Superfrost plus slides (Menzel, Braunschweig, Germany). After drying sections were fixed in ice-cold aceton and dried again. Sections were rehydrated in distilled water, rinsed with PBS and either quenched with H_2O_2 or directly blocked with 10% FCS/Avidin (Vector Laboratories, CA, USA) and than incubated with anti-A6 antibody produced by immunization with an oval-cell enriched liver fraction [29]. A6 antibody was detected with a biotinylated rabbit anti-rat antibody (DAKO, Hamburg, Germany). Sections were further processed with Extravidin-peroxidase conjugate (Sigma). For all other antibodies (Table 1) and for periodic-acid-Schiff (PAS) staining and haematoxylin–eosin (HE) staining 2-μm paraffin sections were dewaxed in Xylol and descending ethanol sequence and rehydrated in distilled water. Antigens were unmasked by microwave treatment and antigen-antibody complexes were detected by peroxidase conjugated secondary antibodies as previously described [25, 30].

Sections used for morphometric analysis of size distribution of nuclei were dewaxed and embedded with Prolong Gold anti-fade reagent containing DAPI (Invitrogen, Karlsruhe, Germany). For PAS staining, used for detection of glycogen in liver tissue, slides were oxidized in 0.5% periodic acid 5 min, rinsed in distilled water, placed in Schiff reagent for 15 min and counterstained after washing in lukewarm tap water in haematoxylin.

Morphometrical analysis

Liver slides were dewaxed, washed in distilled water and equilibrated in TBS. Nuclei of cells were stained with

4'-6-Diamidino-2-phenylindole (DAPI) using Prolong anti-fade reagent containing DAPI (Invitrogen GmbH, Karlsruhe, Germany). Twenty randomly selected visual fields per slide were captured automatically with sensitive greyscale camera (Hamamatsu, Orca 285) using an inverted microscope (Nikon, TE2000) with 20X objective (CFI Planfluor ELWD 20X/0.45). Focus and brightness parameter were calculated by software reducing human influence on image acquisition [31].

The number of cell nuclei was identified using a histogram based mixture model threshold algorithm. Hepatocytes were described on their size between 8 µm x 8 µm and 25 µm x 25 µm and circular shape with index of convexity >0.9 (index of convexity: IC(a) = Area(a)/ConvexArea(a)) and roundness <1.5 (roundness: R(a) = long axis length(a)/short axis length(a)) and quantified in 20 visual fields of 293,260 μm^2 (width: 620 µm, height: 473 µm).

For determining the mitotic index mitotic figures were counted in the right middle lobe and omental lobe of each section of four mice per time point. Area of the lobes was quantified using Axiovision Release 4.5 software after scanning the sections with an Axiovert 200M microscope (Zeiss, Oberkochen, Germany).

Senescence-associated β-galactosidase (SA-β-Gal) staining

Frozen liver samples were cut and mounted on Superfrost plus slides (Menzel). Slides were dried 1 hr at room temperature and fixed with 0.5% glutaraldehyde in PBS 5 min at room temperature. After washing in PBS slides were incubated in citrate buffer (40 mM Na_2HPO_4, 40 mM citrate pH 6,0) stained overnight at 37°C with SA-β-GAL staining solution (1 mg/ml 5-bromo-4-chloro-3-indolyl-β-D-galactoside (X-Gal) in 40 mM citric acid, sodium phosphate, pH 6,0, 5 mM potassium ferrocyanide, 5 mM potassium ferricyanide, 150 mM NaCl and 2 mM $MgCl_2$). Slides were washed in PBS and counterstained with Mayer's haematoxylin.

Results

Inducible expression of transgenic $p16^{INK4a}$ in livers of adult mice

Human $p16^{INK4a}$ cDNA was cloned into the tetracycline-inducible, bi-directional vector pBI-L (Clontech) and used to generate transgenic mice (service of transgenic mouse facility, F. Zimmermann, ZMBH Heidelberg), leading to the production of three lines which stably transmitted the transgene $p_{tet}p16^{INK4a}$. $P16^{INK4a}$ expression was subsequently targeted to the liver by interbreeding each $p_{tet}p16^{INK4a}$ line with the liver-specific TA^{LAP-2} mouse [23] (Fig. 1A). Transgenic $p16^{INK4a}$ expression was prevented during early development by the administration of Dox during mating and throughout pregnancy. Since the pBI-L vector links the expression of $p16^{INK4a}$ to that of luciferase, luciferase activity was used to monitor the level and inducibility of transgene expression in the three lines, revealing that only one of them (U59) was stably inducible on Dox withdrawal (10,000 r.l.u./µg protein compared to 0.1 to 1.0 r.l.u. per µg protein in Dox-treated controls).

On western blots of liver protein, an antibody directed against the C-terminus of human $p16^{INK4a}$ (clone C-20) detected the expected species of 16 kDa in livers of induced transgenic mice but not of Dox-treated mice (Fig. 1B). Two further antibodies directed against the amino terminus (clone N-20) or full length protein (clone G175-405) confirmed these observations but also revealed an additional 14 kD species, which therefore appears to be a proteolytic product of $p16^{INK4a}$ lacking the C-terminus. Interestingly, levels of endogenous $p16^{INK4a}$ slightly decrease upon induction of the transgene, indicative of compensatory regulation.

Immunocytochemical studies revealed transgenic human $p16^{INK4a}$ protein to be localized to both the cytoplasm and the nuclei of expressing cells (Fig. 1C) similar to results described for other cell cycle proteins (for review see [32]). The expression of transgenic $p16^{INK4a}$ did not result in any gross phenotypical changes either in liver or other organs. However, distinct changes were found at the histological level. The hepatocyte nuclei of $p16^{INK4a}$ expressing male mice were both fewer in number and larger in size than those of the controls (Fig. 2), while $p16^{INK4a}$ expressing female mice accumulated fat in hepatocytes and rarely possessed hypertrophic hepatocytes. All subsequent experiments were performed using male mice only. Flow cytometric analysis of propidium iodide stained hepatocytes [33] subsequently confirmed that $p16^{INK4a}$ expressing male mice had an increased proportion of hepatocytes with ploidy > 4N (Fig. 3A and B). Interestingly, the hypertrophic hepatocytes did not themselves

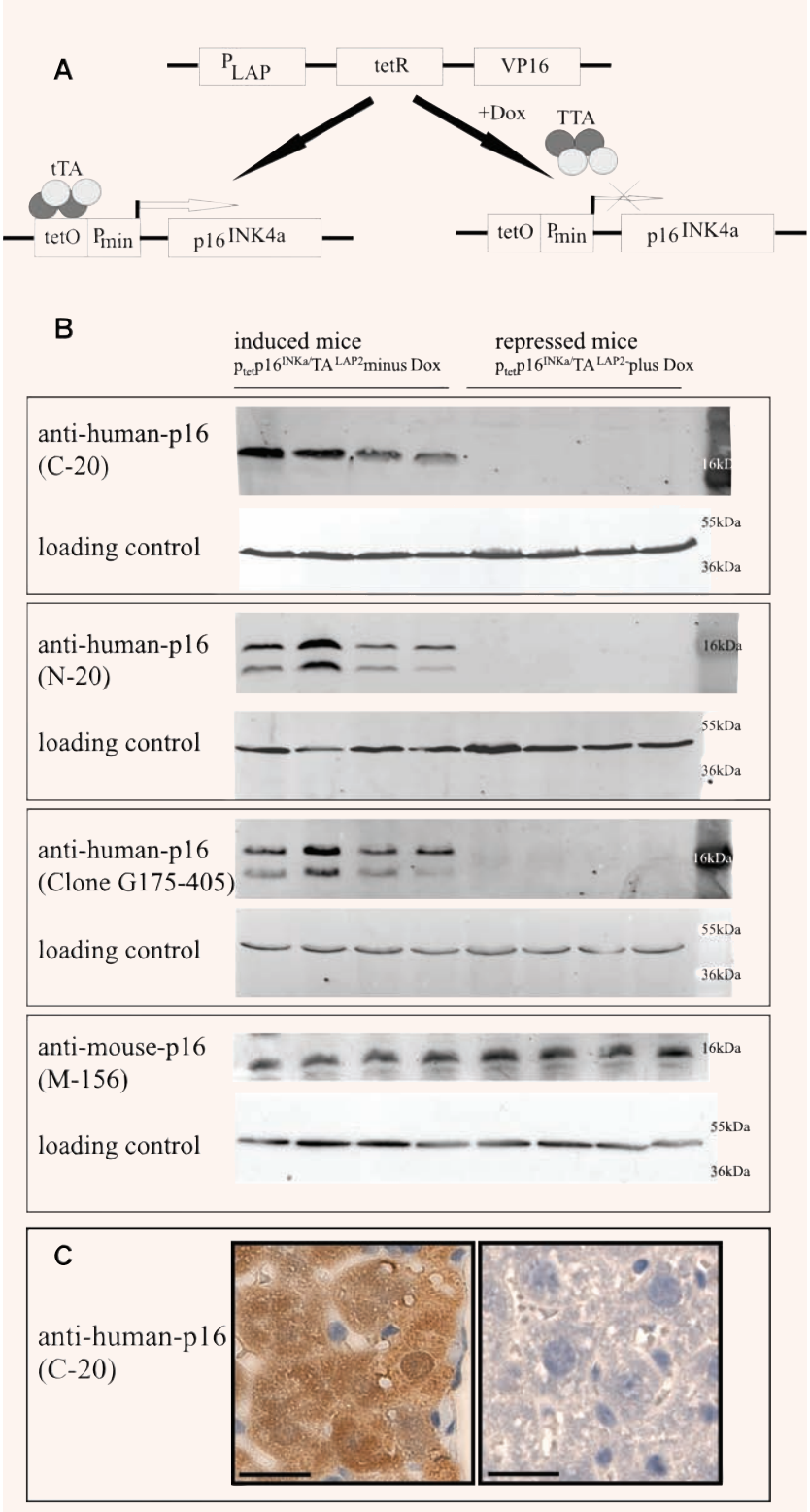

Fig. 1 Conditional liver-specific expression of p16^{INK4a}. (**A**) The transactivator (tTA), a fusion protein of an *Escherichia coli* derived tet repressor (tetR) DNA binding domain and the transactivation domain of VP16 protein derived from herpes simplex virus [62] is placed under the control of a C/EBPβ (LAP) promoter, which allows a hepatocyte-specific expression of the tTA protein. The tTA protein can specifically bind to the tet operator (tetO) sequence and subsequently induces the transcription from the adjacent cytomegalovirus (CMV) minimal promoter which is combined with a transgene (p16^{INK4a}). Tetracycline or its derivative doxycycline (Dox) can prevent binding of tTA to tetO and the transactivation of any transgene cloned behind the CMV promoter is stopped. In contrast, removal of Dox allows the induction of transgene expression. Modified from Gossen *et al.* [63] (**B**) Western blot analysis of human p16^{INK4a} in liver extracts of p_{tet}p16^{INK4a}TA^{LAP-2} mice. Liver extracts of induced male double transgenic p_{tet}p16^{INK4a}TA^{LAP-2} mice (minus Dox) were compared to control liver extracts (plus Dox). Three different p16^{INK4a}antibodies were utilized as indicated and blots were normalized by scanning β-actin as loading control. (**C**) Immunohistochemical staining of mouse liver sections with anti-human p16^{INK4a} antibody. In induced p_{tet}p16^{INK4a}TA^{LAP-2} mice (left photomicrograph) hepatocytes express p16^{INK4a}, detected by the brown colour (DAB staining), which is localized in both cytoplasm and nucleus. Non-parenchymal liver cells and endothelial cells do not express any transgenic protein. No p16^{INK4a} protein was detected in repressed p_{tet}p16^{INK4a}TA^{LAP-2} mice (right photomicrograph). Bar represents 20 μm.

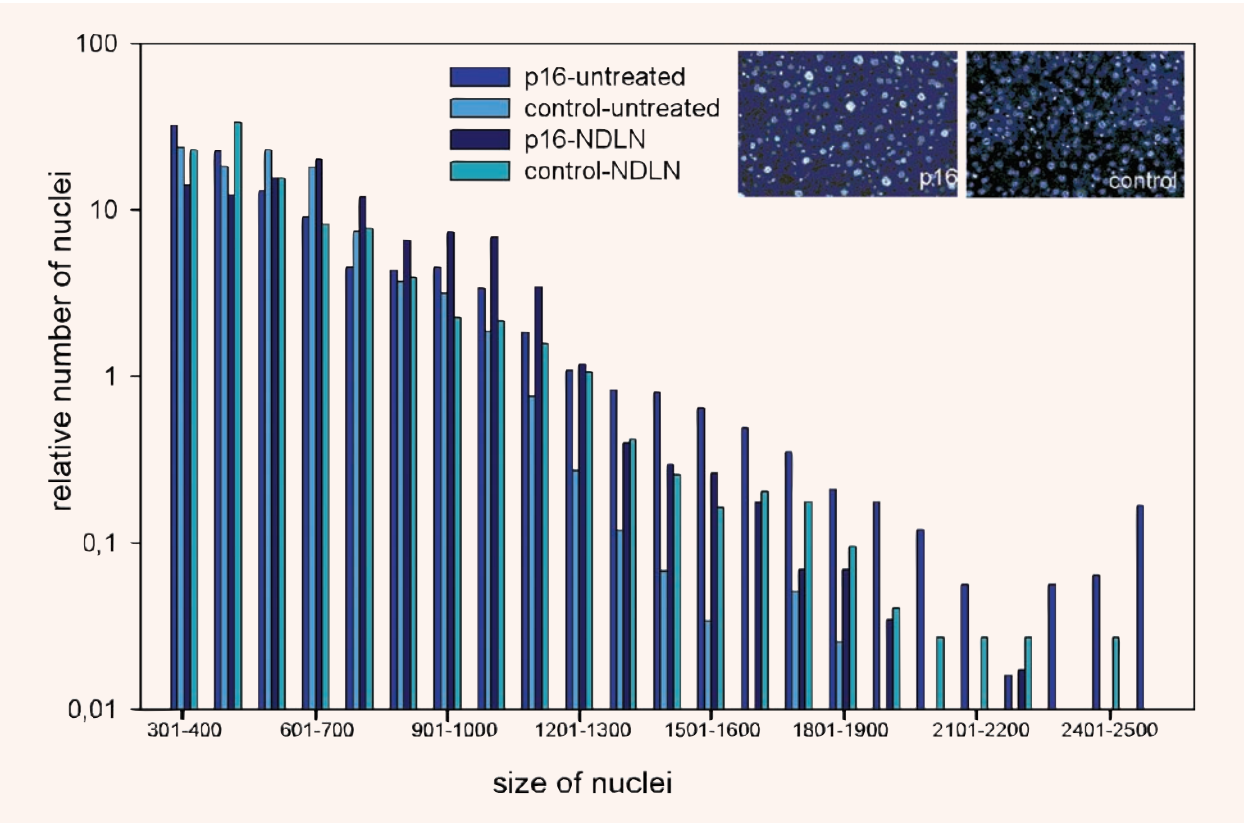

Fig. 2 Size distribution of hepatocyte nuclei in liver slides of $p_{tet}p16^{INK4a}$-TA^{LAP-2} mice and control mice with and without nodularin treatment. Number of hepatocyte nuclei (DAPI stained) identified on their circular shape were quantified. The absolute number of nuclei in this area was 121 ± 30 for controls (with Dox, untreated) and 105±40 for $p16^{INK4a}$ expressing mice (without Dox, untreated) and 74±39 for controls and 62±40 for $p16^{INK4a}$ expressing mice after nodularin treatment (NDLN), respectively. All differences were statistically significant ($P < 0.05$, Student's t-test). For graphical illustration the total number of cells counted in each area was set 100% and the proportion of cells with nuclei of sizes indicated is shown. Liver slides from six control mice and six $p16^{INK4a}$-expressing mice sacrificed at the age of 8 weeks from different litters were quantified. Livers from four control and six $p16^{INK4a}$ expressing mice injected 12 weeks i.p. with nodularin and sacrificed 4 weeks after treatment were used for the quantification.

express detectable levels of transgenic $p16^{INK4a}$ (Fig. 4A1). However, they clearly did demonstrate metabolic activity appropriate to their environment, producing enzymes of nitrogen metabolism (including glutamine synthetase, Fig. 4A2) if localized in the pericentral region of liver lobulus, and carbamoyl phosphate synthetase (Fig. 4A3) if located periportally or midzonally. The hypertrophic hepatocytes also accumulated glycogen in a manner comparable to normal hepatocytes (Fig. 4A4) and expressed both the pericentral-specific detoxification enzyme P450 IIE1 (Fig. 4A5) and E-cadherin (Fig. 4A6) which is an additional marker of periportal hepatocytes [34].

The induction of $p16^{INK4a}$ expression resulted in associated changes in the expression of a number of other genes involved in cell cycle control. Specifically, the levels of $p27^{Kip1}$, cyclin E and CDK6 protein were decreased, while those of cyclin D1 and CDK4 proteins were increased as determined by western blot analysis (Fig. 4B and C). Differences between $p16^{INK4a}$ expressing mice and controls on transcriptional level, measured by microarray

analysis were only marginal (data available at http://www.ebi.ac.uk/arrayexpress/experiments/E-MEXP-1264). Despite the only slight increase of cyclin D1 expression in microarray analysis it was also determined by quantitative RT-PCR (Fig. 7A) to be significantly increased at the level of mRNA, whereas CDK4 mRNA levels quantified also with RT-PCR were equal to controls (data not shown).

P16^{INK4a} expression during early mouse development

The adult mice described above were bred under Dox to avoid the potentially disruptive influence of p16^{INK4a} expression on the rapid developmental expansion and differentiation of liver which starts around embryonic day 10 with expression of C/EBPβ (LAP) [35]. To test whether this is in fact an issue, $_{tet}$p16^{INK4a} and TA^{LAP-2} mice were interbred in the absence of Dox. Luciferase activity was detectable by embryonic day 12, being the earliest time point tested. Pups were born apparently normally, and the expression levels of both luciferase and p16^{INK4a} in neonates (Fig. 5A, B, and C) were comparable to those found in adult mice following discontinuation of Dox. The livers of adult mice bred and maintained in the absence of Dox displayed the same histological features as those of mice withdrawn from Dox either at birth or after weaning, demonstrating that the embryonic overexpression of p16^{INK4a} has no marked consequences for liver development. However, the livers of neonatal and weaning mice (14 days) expressing p16^{INK4a} were characterised by the overexpression around portal vessels of E-cadherin (Fig. 5D1, D3), which might correspond to progenitor cells [36].

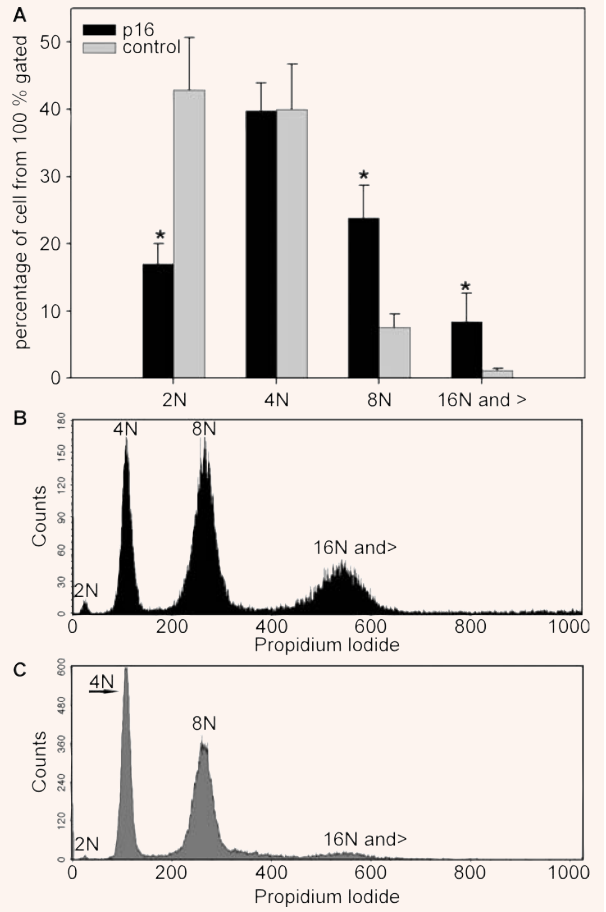

Fig. 3 Flow cytometric analysis of propidium iodide stained hepatocytes. (**A**) The proportions of cells with diploid (2N), tetraploid (4N), octaploid (8N) and hexadecaploid and higher (16N and >) DNA content were analysed as percentage of cells from 100% gated. Significant differences $P < 0.02$ between p16^{INK4a} expressing livers and controls were labelled with an asterisk. Representative histograms of FACS analysis of a unique p16^{INK4a} expressing liver (**B**) and control (**C**) are depicted.

Actions of proliferative stimuli on p16^{INK4a} expressing adult livers

Partial hepatectomy

(PH) firstly described by Higgins and Anderson [37] is the strongest known stimulus for liver regeneration, with a two-third PH recruiting almost all hepatocytes into cycle within 48 hrs [17], so that an average of less than two doublings is sufficient to restore hepatocyte numbers. As expected, a 2/3 hepatectomy of control mice resulted in rapid activation of hepatocytes and the regeneration of 100% over 14 days. Interestingly, the mitotic index (MI) of hepatocytes in mice expressing p16^{INK4a} was slightly higher than that in the controls from 48 hrs after PH, equal in both groups 72 hrs after PH, but significantly increased in livers of induced mice 14 days after PH (p16^{INK4a} expressing mice display a MI of 9.9 per 50 mm^2 and controls show 1 per 50 mm^2). The mitotic figures, few of them visible as triphasic spindles, were restricted to cells which showed no detectable

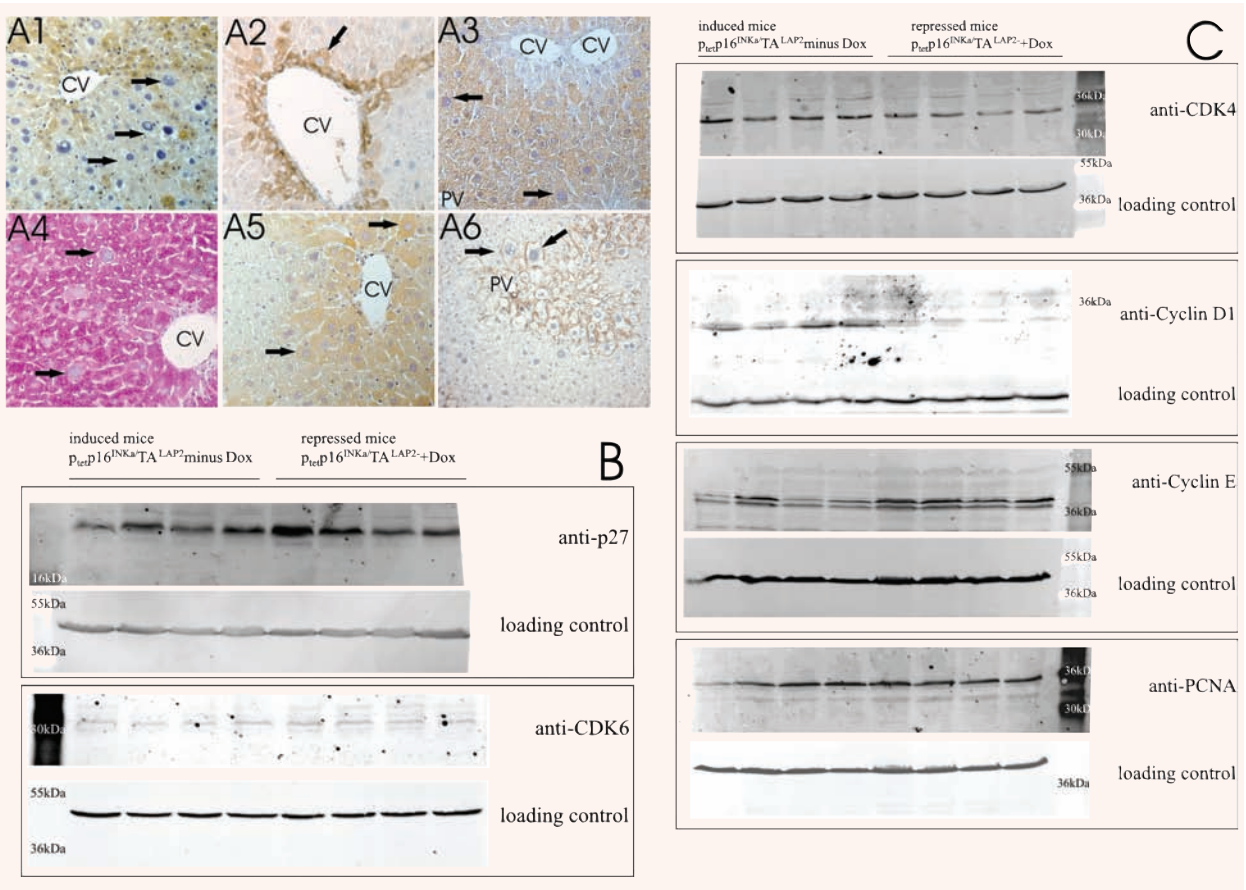

Fig. 4 Expression of cell cycle proteins in liver extracts of $p_{tet}p16^{INK4a}TA^{LAP-2}$ mice and histological features of livers of $p16^{INK4a}$ expressing mice. (**A**) Photomicrographs of liver slides. $P16^{INK4a}$ protein was detected in hepatocytes of induced $p_{tet}p16^{INK4a}TA^{LAP-2}$ mice with an anti-human $p16^{INK4a}$ antibody (C-20) (**A1**, brown colour). In livers of male $p16^{INK4a}$ expressing mice many of enlarged hepatocytes were observed (**A1**-**A6**, black arrows). These hepatocytes do not express $p16^{INK4a}$ (**A1**) but express liver region-specific proteins like glutamine synthetase (**A2**) and cytochrome-P450 IIE (**A5**) representing pericentrally specific enzymes and carbamoyl phosphate synthase (**A3**), and E-cadherin (**A6**) being marker proteins for periportal and midzonal hepatocytes and also store glycogen (**A4**, pink colour). Proteins were detected with primary antibodies and immunocomplexes were visualized by DAB staining (brown). Bars represent 50 μm; CV, central vein; PV, portal vein (**B**, **C**) Western blots with antibodies against cell cycle proteins in liver extracts of induced (minus Dox) respectively switched off (+Dox) $p_{tet}p16^{INK4a}TA^{LAP-2}$ mice.

$p16^{INK4a}$ staining (Fig. 6). Bearing in mind the reduced regenerative capacity in these animals, it seems likely that these cells undergo either a retarded mitosis or most probably a prolonged proliferative response compensating for the low frequency of recruitable (non-expressing) hepatocytes similar as shown in the telomerase knock-out model [38]. This proliferation of $p16^{INK4a}$ non-expressing hepatocytes was obviously sufficient to restore liver mass after the unique proliferative stimulus by PH. Livers of induced mice were checked up on oval cell proliferation at several time points (48 hrs, 3, 4, 6, 7, 12 and 14 days after PH) but never a recruitment of facultative stem cell compartment was observed (data not shown).

Nodularin treatment

Nodularin, a natural heptapeptide produced by *Cyanobacteria*, is an inhibitor of protein phosphatases 1/2A (PP1/2A) and has strong liver specificity resulting from the route of uptake *via* the

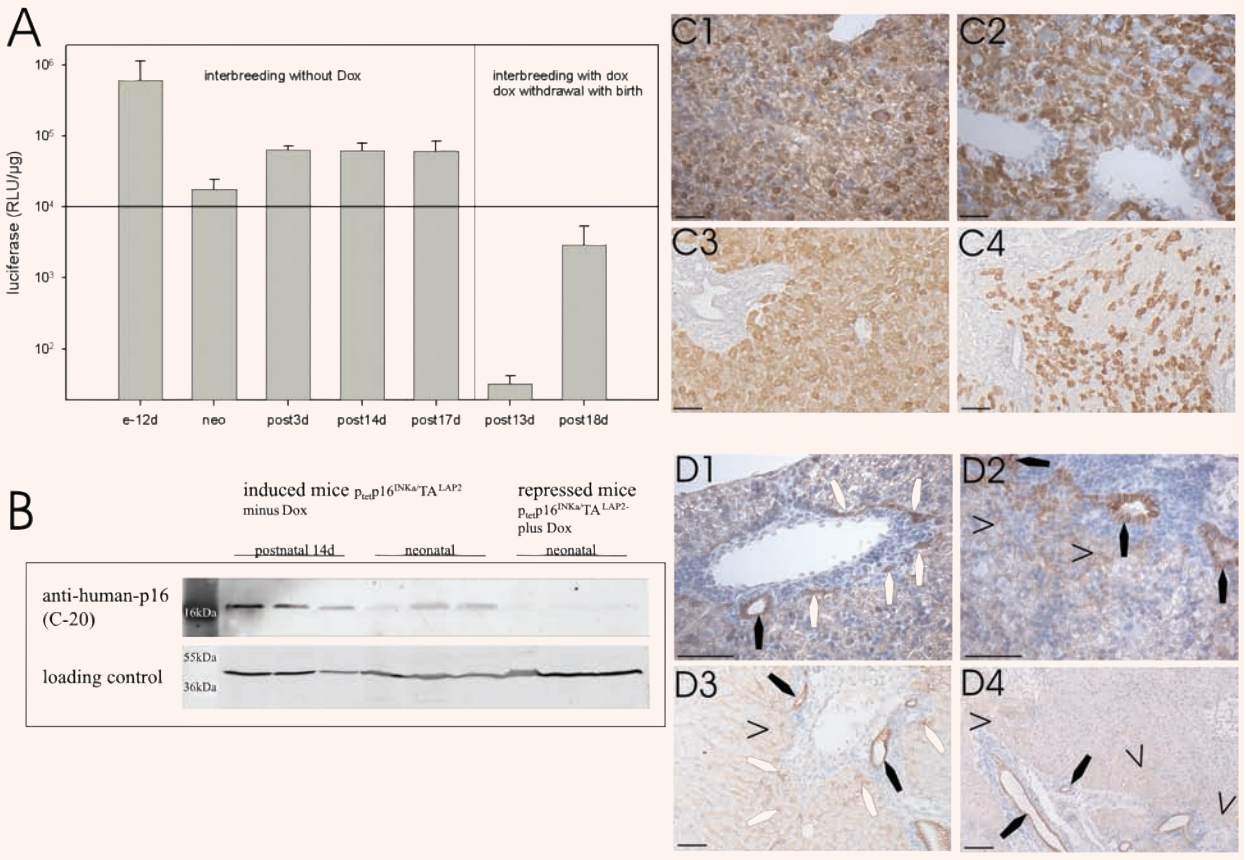

Fig. 5 Induction of gene expression in early liver development. Inter-breedings of $p_{tet}p16^{INK4a}$ mice with the liver specific TA^{LAP-2} mice were performed without Dox or with Dox as indicated. (**A**) Luciferase activity was measured in liver extracts of foetal mice (e-12d, 12 days postinsemination), neonatal mice (neo) and postnatal mice (post14d, post13d, post17d and post18d). The solid line represents the mean values of luciferase measured in adult mice. (**B**) $P16^{INK4a}$ expression was checked by western blotting in neonatal and postnatal mice with the anti-human p16 antibody (C-20). Anti-β-actin antibody was used as loading control. (**C**) Paraffin sections of livers of neonatal (**C1**, **C2**) and 14-day-postnatal mice (**C3**, **C4**) were incubated with anti-p16 antibody (C-20) and immunocomplexes were visualized with an peroxidase conjugated secondary antibody and DAB staining (brown). Expression levels of the four representatively depicted $p16^{INK4a}$ expressing mice vary individually, despite comparatively high luciferase activities. (**D**) Anti-E-cadherin immunoreactivity on paraffin sections of livers of neonatal (**D1**, **D2**) and postnatal (14d) mice. $P16^{INK4a}$ expressing mice (**D1**, **D3**) were compared to controls (**D2**, **D4**). Pronounced expression of E-cadherin around portal vessels were detected in $p16^{INK4a}$ expressing mice (**D1**, **D3,** white polygon), but not observed in liver slides of control mice (**D2**, **D4**). E-cadherin was expressed in periportal hepatocytes (arrow heads) and cholangiocytes (black polygon) like in adult mice. Bar represents 50 µm.

multi-specific bile acid transport system which occurs only in hepatocytes [39–41]. Since PP1/2A activity is required for the de-phosphorylation of RB at the end of mitosis [42], inhibition of PP1/2A should prolong the proliferative response in all cells capable of phosphorylating RB. Indeed, the promoting effect of nodularin on hepatocyte proliferation has previously been shown in rat liver by proliferating cell nuclear antigen (PCNA) staining [43]. In our inducible transgenic model, those hepatocytes which express $p16^{INK4a}$ should not phosphorylate RB, and should therefore be indifferent to PP1/2A inhibition. Here, the proliferation of non-$p16^{INK4a}$ expressing cells, including the liver-specific stem cells would be expected to be stimulated preferentially by nodularin treatment. Indeed after treatment livers of induced mice show

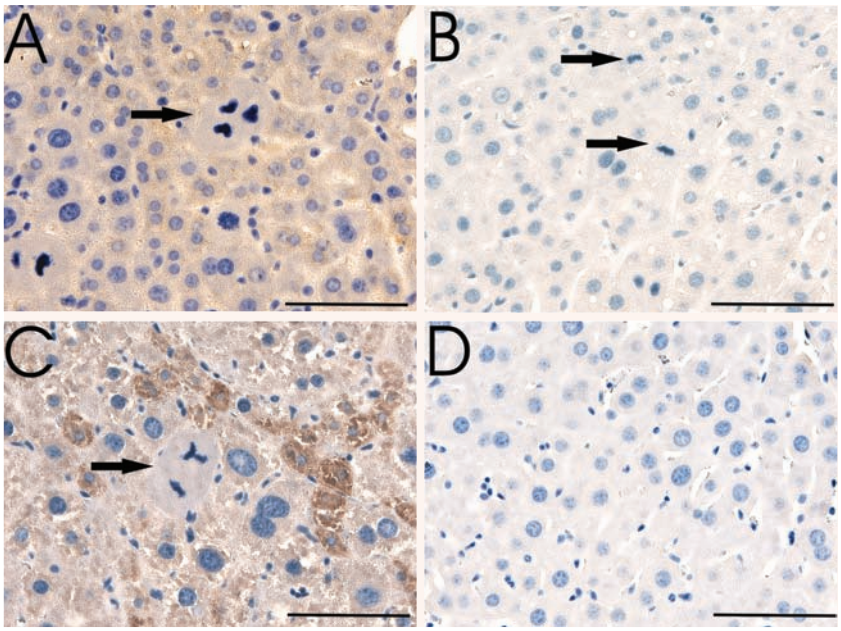

Fig. 6 Mitotic figures in mouse liver sections after partial hepatectomy. (**A**) Sections of mouse livers of induced $p_{tet}p16^{INK4a}TA^{LAP-2}$ mice (**A**, **C**) and control mice (**B**, **D**) were stained with the anti-$p16^{INK4a}$ antibody (C-20, yellowish-brown colour) 72 hrs (**A**, **B**) and 14 days (**C**, **D**) after PH. Mitotic figures were identified by chromosomes visible as tangled, dark-staining threads (arrows). Number of mitotic figures in $p16^{INK4a}$ expressing and non-expressing livers was similar 72 hrs after PH, but differed significantly 14 days after PH (with control mice having no but $p16^{INK4a}$ expressing mice displaying some mitotic figures 14 days after PH (**C**)). Only in $p16^{INK4a}$ expressing mice abnormal mitotic figures like triphasic spindles were observed. Bar represents 50 μm.

large loci of $p16^{INK4a}$ negative hypertrophic hepatocytes (Fig. 7C2) never seen in untreated livers and a lot of small oval cells which were also $p16^{INK4a}$ negative in immunohistochemical stainings of transgenic $p16^{INKa}$. Nodularin increases the proportion of larger nuclei in control mice, but slightly shifts the ratios in those expressing $p16^{INK4a}$ (Fig. 2) resulting in a total number of hepatocytes per area of 74±39 for controls and 62±40 in $p16^{INK4a}$ expressing mice. The differences between all for groups, control-untreated, $p16^{INK4a}$-untreated and the two nodularin treated groups were statistical significant ($P < 0.05$).

The ability of nodularin to promote proliferation in the livers of control and induced transgenic mice was assessed by quantitative analysis of cyclin D1 mRNA levels and by PCNA staining of liver sections. As expected, nodularin increased hepatocyte proliferation in control mice, leading to increases in the levels of both cyclin D1 mRNA (Fig. 7A) and PCNA staining of hepatocytes (Fig. 7B2). In the induced mice, the comparatively high baseline level of cyclin D1 mRNA was not increased further by nodularin treatment. The PCNA staining pattern in induced mice was clearly different to that of the controls, with weak staining of occasional hypertrophic hepatocytes (Fig. 7B1) and loci of hypertroph hepatocytes (Fig. 7C1) and predominant staining of small, oval shaped cells which we also found to express the oval cell marker A6 (Fig. 7B1 and B3), suggesting that nodularin treatment of the transgenic mice does indeed recruit a population of hepatic stem cells to proliferation. Further immunocytochemical analysis revealed the population of activated oval cells to over-express the epithelial cell marker E-cadherin (Fig. 7B5) that represents another surface marker of oval cells [36]. Oval cells were isolated from $p16^{INK4a}$ expressing mice by collagenase perfusion followed by Percoll gradient centrifugation. The developing cell clones, which were A6 positive to 90% (Fig. 7D1), immediately following isolation, were removed from the culture flask by trypsin- treatment and expanded. These cells remained the high level expression of A6-antigen over approximately 10 passages (Fig. 7D2). Further culture resulted in a progressive reduction in reactivity (Fig. 7D3). Four lines (OVUE265, OVUE867, OVUE869 and OVUE871) individually isolated from independent preparations were expanded and cryopreserved. The same experimental procedure was used in parallel for control mice but did not result in expandable cells.

Three of the four lines (OVUE867, 869 and 871) were derived from triple transgenic mice carrying an EGFP marker appropriate for subsequent transplantation experiments. None of the lines express either $p16^{INK4a}$ protein or luciferase activity, consistent with the complete silencing of C/EBPβ (LAP) in oval cells. These lines should therefore provide an excellent tool for monitoring activation of the C/EBPβ (LAP)

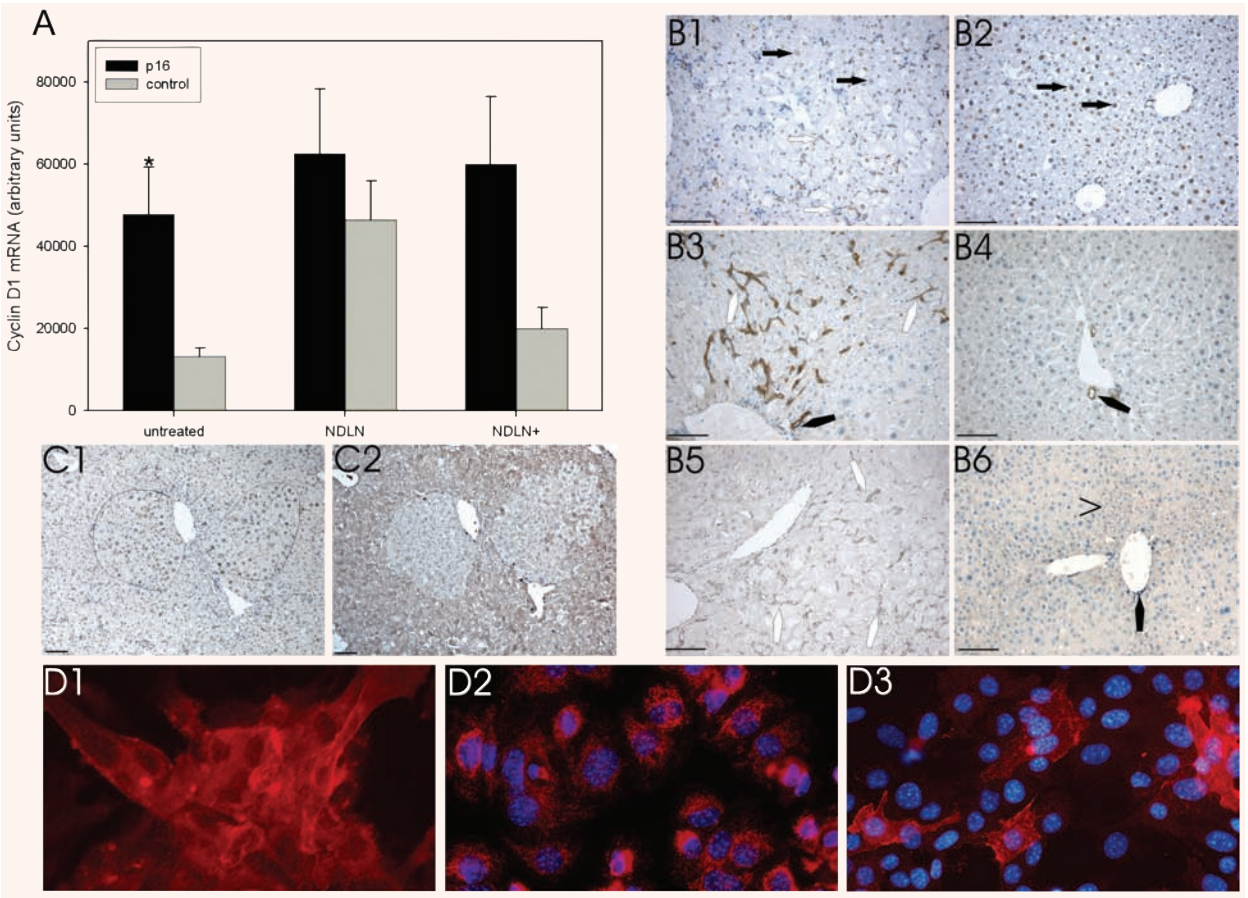

Fig. 7 Liver-specific stimulation of proliferation by nodularin. Mice were treated with nodularin thrice weekly and killed next day after the last injection (NDLN) or 4 weeks after the last injection ($NDLN^{+}$). (**A**) Cyclin D1 mRNA levels were determined by real time RT-PCR. Differences between untreated $p16^{INK4a}$ expressing and control mice, between controls and NDLN-treated controls (NDLN), and between nodularin treated controls that were killed 4 weeks after NDLN treatment were statistically significant ($P < 0.05$, Student's t-test). The number of different animals tested was: p16(untreated) = 7, control(untreated) = 5, p16(NDLN) = 8, control(NDLN) = 12, $p16(NDLN^{+}) = 21$, control ($NDLN^{+}$) = 12. (**B**) *in situ* immunodetection of PCNA (**B1**, **B2**), A6 antigen (**B3**, **B4**) and E-Cadherin (**B5**, **B6**) in nodularin treated mice. 80-90% of hepatocytes nuclei of control mice were immunostained with the PCNA antibody (brown colour, **B2**). In $p16^{INK4a}$ expressing mice predominantly small cells with oval nuclei were positively stained with the PCNA antibody (white arrow) and some of the hypertrophic hepatocytes (**B1**, black arrows), but less intensive than hepatocytes in control mice (**B2**, black arrows). The anti-A6 antibody identifies these cells as facultative liver stem cells, oval cells, forming ductular structures (**B3**, white polygon). These bipotent facultative stem cells of liver express the A6 antigen like cells of the biliary system (cholangiocytes, **B3**, **B4**, black polygon). A common feature of epithelial cells, hepatocytes, cholangiocytes and oval cells, in liver is the expression of E-cadherin. On the histological level E-cadherin is detected in periportal hepatocytes (**B6**, black arrowhead) biliary ductuli (**B5**, **B6**, black polygon) and oval cells (**B5**, white polygons), whereas the latter form the same ductular structures detected with the A6 antibody (**B3**). (**C**) Nodularin treated $p16^{INK4a}$ expressing mice (**C1**, **C2**) develop $p16^{INK4a}$ negative loci (**C2**) consisting of accumulating hypertrophic hepatocytes. Some of the hypertrophic hepatocytes were PCNA positive (**C1**, brown). The black lines mark the two foci in the PCNA stained liver slide (**C1**). (**D**) Oval cells were isolated from nodularin treated $p16^{INK4a}$ expressing mice by two-step collagenase perfusion and subsequently density gradient centrifugation. A6-positive cells (red colour) of passage 0 (**D1**) growing clonally were trypsinated and cultured to passage 10 (**D2**) without loss of A6 antigen. In higher passages (**D3**, passage 16) a loss or down-regulation of A6 expression was observed. Representative photomicrographs of OVUE265 are displayed. Bar represents 50 μm.

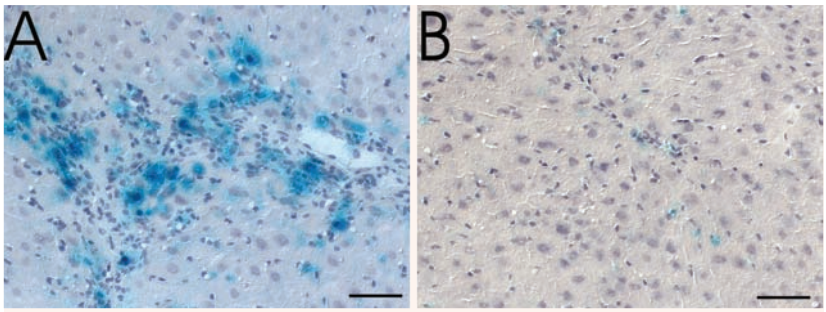

Fig. 8 Enzyme histochemical detection of senescence-associated β-galactosidase. Eight weeks old $p16^{INK4a}$ expressing mice (**A**) and control mice (**B**) were treated with nodularin for a period of 12 weeks and killed 5 days after treatment. SA-β-Gal (light blue colour) was expressed mainly in hepatocytes. Bar represents 50 μm.

promoter *via* reporter enzyme luciferase induction during differentiation of oval cells into mature hepatocytes under *in vitro* and *in vivo* conditions.

Interval feeding

The proliferation of hepatocytes is strongly responsive to feeding rhythms [44] and a repeated interval-feeding (2d-starvation, 1d-refeeding, 10-cycles) leads to synchronized cell cycling and increased hepatocyte renewal to replace cells lost through frequent apoptotic events during the starvation phases [25, 45]. It was therefore of interest to determine whether interval feeding resulted in the recruitment of hepatic stem cells to proliferation. No activation of oval cells was detected either in control (uninduced) mice or in young (less than 8 weeks) induced mice subject to interval feeding. However, oval cell activation was detected by both A6 and E-cadherin immunohistochemistry (data not shown) in 100% of interval-fed induced mice over 8 months of age. This frequency was reduced to 66% when Dox was re-administered during the period of interval feeding. The recruitment of oval cells to proliferation is therefore a function of both $p16^{INK4a}$ expression and age, associated most probably with cumulative proliferative demand.

Expression of senescence-associated β-galactosidase

Physiological $p16^{INK4a}$ overexpression is associated with senescence [46] and is frequently accompanied by expression of senescence-associated β-galactosidase (SA-β-Gal) both in cultured cells [47, 48] and in liver *in situ* [49]. The age-related effects of $p16^{INK4a}$ expression revealed by interval feeding raise the question of whether $p16^{INK4a}$ is merely a marker of senescence or may actively promote senescence processes. To test this, we determined the expression level of SA-β-Gal *in situ.* We found equal levels of SA-β-Gal in the livers of $p16^{INK4a}$ expressing and control mice, either in the quiescent state (without any treatment) or following PH. In contrast, strong up-regulation of SA-β-Gal was detected in $p16^{INK4a}$ expressing livers both in nodularin-treated and interval-starved mice, both treatments being associated with recruitment of oval cells. Indeed, the most intensive staining for SA-β-Gal was detected in hepatocytes of livers with the highest numbers of oval cells (Fig. 8A).

Discussion

We report the derivation and characterisation of transgenic mice in which the physiological cell cycle inhibitor $p16^{INK4a}$ is expressed in hepatocytes in an inducible fashion. The aim of this exercise was to increase the proliferative demand on hepatic stem cells by blocking the proliferation of hepatocytes which occurs as a first-line response to liver damage.

The induction of $p16^{INK4a}$ expression in adult liver hepatocytes had no obvious pathological consequences. However, at the histological level there was an increase in polyploidy and the appearance of hypertrophic hepatocytes, being indicative of increased maturation and compromised cell division [50] respectively. Interestingly, the hypertrophic hepatocytes characteristic of $p16^{INK4a}$ expressing livers did not themselves express detectable levels of $p16^{INK4a}$ protein. This suggests that hypertrophy occurs through a pathway dependent on $p16^{INK4a}$, but that expression is inactivated prior to or during hypertrophic growth, possibly reflecting a selection for non-expressing cells. The hyperploidy in these hepatocytes is a sign of premature senescence and points to the former expression of $p16^{INK4a}$. A second

rather unlikely hypothesis might suppose a generation of p16-negative hepatocytes from oval cells in a direct way avoiding any expression of transgenic $p16^{INK4a}$ during their lifetime. This strategy would exclude the C/EBPβ (LAP) promoter activation, which (*i*) is a prerequisite for expression of transgenic $p16^{INK4a}$, but (*ii*) is also an essential event during normal hepatocytes differentiation process. But in our study the hypertroph/hyperploid p16-negative hepatocytes display normal hepatocytic markers, indicating a normal hepatocytic development. Against the background of compromised hepatocyte proliferation in adult, we found that hepatic stem (oval) cells could indeed be recruited by two independent stimuli: nodularin treatment (which should extend the proliferative response of replication competent cells that do not express $p16^{INK4a}$); and interval feeding (which both increases and synchronizes proliferative demand due to hepatocyte apoptosis during the starvation phases). We found the recruitment of oval cells by an interval-feeding regime to be dependent not only on the expression of $p16^{INK4a}$ in hepatocytes but also on advancing age of the mouse. This suggests that the mechanisms of regeneration may differ markedly between young and old mice and/or that oval cells tend to respond to cumulative proliferative demand over extended periods. We favour the latter interpretation firstly since the response to nodularin confirms the presence and responsivity of oval cells in young mice, and secondly because of our surprising finding that neither the acute proliferative response of adult hepatocytes to PH, nor the rapid growth of liver during foetal development were strongly compromised by $p16^{INK4a}$ expression. There may therefore be fundamental differences in the mechanisms of regeneration in response to chronic/extensive and acute/intensive damage, perhaps reflecting the different requirements for the replacement of isolated cells on the one hand and of entire functional units on the other.

We show herein that accumulation of transgenic $p16^{INK4a}$ restricts the regenerative capacity of hepatocytes and enforces the activation of facultative stem cell compartment of liver, being $p16^{INK4a}$ negative, when repeated proliferation is required like in the nodularin- and interval-feeding model. This verifies the limited role of $p16^{INK4a}$ in normal development as shown in $p16^{INK4a}$ null mice [3, 4] and its pivotal role in critical situations influencing the tissue homeostasis. Otherwise it was shown that growth-constrained environment can select for outgrowth and malignant transformation of hepatocytes [51, 52] and $p16^{INK4a}$ overexpression was described in invasion front of carcinomas [53]. This could result in selection of cells with malignant potential. However, our study show that neither the $p16^{INK4a}$ negative hepatocytes nor oval cells that developed in liver after proliferative stimuli possess an increased proliferative potential after removing the stimulus. Both livers of nodularin treated and untreated transgenic mice weighed slightly lesser than control livers and tumours were never observed actually after expression of $p16^{INK4a}$ over several month up to one year.

It is remarkable, that during liver development overexpression of $p16^{INK4a}$ did not cause dramatic effects. This would hardly be explainable on the basis of the classical understanding of cell cycle where such increased $p16^{INK4a}$ expression should completely arrest hepatocytic proliferation. However, recently, results obtained from CDK4 and CDK6 null mouse embryos [54] show normal organogenesis and cell proliferation levels, indicating, that the function of CDK4 and CDK6 can be accomplished at least temporarily (or locally in definite compartments) by other CDKs, *i.e.* CDK2, supporting a hypothesis that lacking of specific CDKs, cyclins or inhibitors can be compensated for by alternative mechanisms during various phases of development [55–58]. This also could explain the rather normal development of livers in our transgenic mice, with only limited involvement of alternative strategies.

Nevertheless, the fact that the overexpression of $p16^{INK4a}$ during development results in increased polyploidy and E-cadherin overexpression even in neonates suggests that oval cells are recruited in these mice from an early stage. The lack of pathology in these mice even at advanced age therefore supports the robust, normal function of oval cell derived hepatocytes in the long term and their potential relevance for regenerative therapy.

With a view to defining strategies for the cell therapy of chronic liver damage in humans it will therefore be important to define the mechanisms underlying the recruitment, proliferation and differentiation of oval cells. In this respect, our results provide an important proof of principle that oval cells can indeed be recruited by a combination of CDK inhibition (in our case *via* the expression of $p16^{INK4a}$) and a non-cytotoxic interval-feeding regime. The silencing of C/EBPβ promoter in oval cells in our mouse model confirms the strong hepatocyte specificity of the

used promoter [23, 30] and data obtained during differentiation of a transformed liver progenitor cell line of foetal mouse liver [59], but are in contrast to *in situ* data from rat experiments that show the expression of C/EBPβ in a subpopulation of oval cells [60]. The reason of the inconsistent data might be differences in expression pattern of oval cells in rat and mouse, recently strikingly shown by Jelnes and coworkers [61].

The oval cell lines isolated in this study, all of which carry both luciferase and $p16^{INK4a}$ under the control of the hepatocyte-specific C/EBPβ promoter (which is obviously inactive in the progenitor oval cell stage) and three of which are tagged additionally with GFP, will provide a valuable tool to analyse the regenerative potential of the recruited population both *in vitro* and *in vivo*.

Acknowledgements

We thank Natalia Engelhardt (Kolzow Institute, Moscow) for providing of A6 antibody. We also thank Martina Fügenschuh, Institute of Pathology, University of Leipzig for embedding tissue. This study was supported by Interdisciplinary Centre for Clinical Research at the Medical Faculty of the University of Leipzig (01KS9504, Project C1).

References

1. **Sherr CJ, Roberts JM.** Inhibitors of mammalian G1 cyclin-dependent kinases. *Genes Dev.* 1995; 9: 1149–63.
2. **Zindy F, Quelle DE, Roussel MF, Sherr CJ.** Expression of the $p16^{INK4a}$ tumor suppressor *versus* other INK4 family members during mouse development and aging. *Oncogene.* 1997; 15: 203–11.
3. **Krimpenfort P, Quon KC, Mooi WJ, Loonstra A, Berns A.** Loss of $p16^{INK4a}$ confers susceptibility to metastatic melanoma in mice. *Nature.* 2001; 413: 83–6.
4. **Sharpless NE, Bardeesy N, Lee KH, Carrasco D, Castrillon DH, Aguirre AJ, Wu EA, Horner JW, DePinho RA.** Loss of $p16^{INK4a}$ with retention of p19Arf predisposes mice to tumorigenesis. *Nature.* 2001; 413: 86–91.
5. **Sharpless NE, Ramsey MR, Balasubramanian P, Castrillon DH, DePinho RA.** The differential impact of p16(INK4a) or p19(ARF) deficiency on cell growth and tumorigenesis. *Oncogene*. 2004; 23: 379–85.
6. **Sharpless NE.** ^{INK4a}/Arf links senescence and aging. *Exp Gerontol*. 2004; 39: 1751–9.
7. **Chimenti C, Kajstura J, Torella D, Urbanek K, Heleniak H, Colussi C, Di Meglio F, Nadal-Ginard B, Frustaci A, Leri A, Maseri A, Anversa P.** Senescence and death of primitive cells and myocytes lead to premature cardiac aging and heart failure. *Circ Res.* 2003; 93: 604–13.
8. **Arendt T, Rodel L, Gartner U, Holzer M.** Expression of the cyclin-dependent kinase inhibitor p16 in Alzheimer's disease. *Neuroreport.* 1996; 7: 3047–9.
9. **Luth HJ, Holzer M, Gertz HJ, Arendt T.** Aberrant expression of nNOS in pyramidal neurons in Alzheimer's disease is highly co-localized with p21ras and $p16^{INK4a}$. *Brain Res.* 2000; 852: 45–55.
10. **Ruas M, Peters G.** The $p16^{INK4a}$/CDKN2A tumor suppressor and its relatives. *Biochim Biophys Acta.* 1998; 1378: F115–77.
11. **Herath NI, Leggett BA, MacDonald GA.** Review of genetic and epigenetic alterations in hepatocarcinogenesis. *J Gastroenterol Hepatol.* 2006; 21: 15–21.
12. **Matsuda Y, Ichida T, Matsuzawa J, Sugimura K, Asakura H.** p16(INK4) is inactivated by extensive CpG methylation in human hepatocellular carcinoma. *Gastroenterology.* 1999; 116: 394–400.
13. **Shim YH, Park HJ, Choi MS, Kim JS, Kim H, Kim JJ, Jang JJ, Yu E.** Hypermethylation of the p16 gene and lack of p16 expression in hepatoblastoma. *Mod Pathol.* 2003; 16: 430–6.
14. **Pascale RM, Simile MM, De Miglio MR, Muroni MR, Calvisi DF, Asara G, Casabona D, Frau M, Seddaiu MA, Feo F.** Cell cycle deregulation in liver lesions of rats with and without genetic predisposition to hepatocarcinogenesis. *Hepatology.* 2002; 35: 1341–50.
15. **Pascale RM, Simile MM, Calvisi DF, Frau M, Muroni MR, Seddaiu MA, Daino L, Muntoni MD, De Miglio MR, Thorgeirsson SS, Feo F.** Role of HSP90, CDC37, and CRM1 as modulators of P16(INK4a) activity in rat liver carcinogenesis and human liver cancer. *Hepatology.* 2005; 42: 1310–9.
16. **Steer CJ.** Liver regeneration. *FASEB J.* 1995; 9: 1396–400.
17. **Michalopoulos GK, DeFrances MC.** Liver regeneration. *Science.* 1997; 276: 60–6.
18. **Thorgeirsson SS.** Hepatic stem cells in liver regeneration. *FASEB J.* 1996; 10: 1249–56.
19. **Fausto N.** Liver regeneration. *J Hepatol.* 2000; 32: 19–31.
20. **Roskams T.** Different types of liver progenitor cells and their niches. *J Hepatol.* 2006; 45: 1–4.
21. **Forbes S, Vig P, Poulsom R, Thomas H, Alison M.** Hepatic stem cells. *J Pathol.* 2002; 197: 510–8.

22. **Baron U, Bujard H.** Tet repressor–based system for regulated gene expression in eukaryotic cells: principles and advances. *Methods Enzymol.* 2000; 327: 401–21.
23. **Kistner A, Gossen M, Zimmermann F, Jerecic J, Ullmer C, Lubbert H, Bujard H.** Doxycycline-mediated quantitative and tissue-specific control of gene expression in transgenic mice. *Proc Natl Acad Sci USA.* 1996; 93: 10933–8.
24. **Okabe M, Ikawa M, Kominami K, Nakanishi T, Nishimune Y.** 'Green mice' as a source of ubiquitous green cells. *FEBS Lett.* 1997; 407: 313–9.
25. **Ueberham E, Arendt E, Starke M, Bittner R, Gebhardt R.** Reduction and expansion of the glutamine synthetase expressing zone in livers from tetracycline controlled TGF–beta1 transgenic mice and multiple starved mice. *J Hepatol.* 2004; 41: 75–81.
26. **Greene AK, Puder M.** Partial hepatectomy in the mouse: technique and perioperative management. *J Invest Surg.* 2003; 16: 99–102.
27. **Burger HJ, Gebhardt R, Mayer C, Mecke D.** Different capacities for amino acid transport in periportal and perivenous hepatocytes isolated by digitonin/collagenase perfusion. *Hepatology.* 1989; 9: 22–8.
28. **Arendt E, Ueberham U, Bittner R, Gebhardt R, Ueberham E.** Enhanced matrix degradation after withdrawal of TGF-beta1 triggers hepatocytes from apoptosis to proliferation and regeneration. *Cell Prolif.* 2005; 38: 287–99.
29. **Engelhardt NV, Factor VM, Yasova AK, Poltoranina VS, Baranov VN, Lasareva MN.** Common antigens of mouse oval and biliary epithelial cells. Expression on newly formed hepatocytes. *Differentiation.* 1990; 45: 29–37.
30. **Ueberham E, Low R, Ueberham U, Schonig K, Bujard H, Gebhardt R.** Conditional tetracycline-regulated expression of TGF–beta1 in liver of transgenic mice leads to reversible intermediary fibrosis. *Hepatology.* 2003; 37: 1067–78.
31. **Hiemann R, Hilger N, Sack U, Weigert M.** Objective quality evaluation of fluorescence images to optimize automatic image acquisition. *Cytometry A.* 2006; 69: 182–4.
32. **Ueberham U, Arendt T.** The expression of cell cycle proteins in neurons and its relevance for Alzheimer's disease. *Curr Drug Targets CNS Neurol Disord.* 2005; 4: 293–306.
33. **Mayhew CN, Bosco EE, Fox SR, Okaya T, Tarapore P, Schwemberger SJ, Babcock GF, Lentsch AB, Fukasawa K, Knudsen ES.** Liver-specific pRB loss results in ectopic cell cycle entry and aberrant ploidy. *Cancer Res.* 2005; 65: 4568–77.
34. **Butz S, Larue L.** Expression of catenins during mouse embryonic development and in adult tissues. *Cell Adhes Commun.* 1995; 3: 337–52.
35. **Westmacott A, Burke ZD, Oliver G, Slack JMW, Tosh D.** C/EBPalpha and C/EBPbeta are markers of early liver development. *Int J Dev Biol.* 2006; 50: 653–7.
36. **Ueberham E, Aigner T, Ueberham U, Gebhardt R.** E-cadherin as a reliable cell surface marker for the identification of liver specific stem cells. *J Mol Histol.* 2007; 38: 359–68.
37. **Higgins GM, Anderson RM.** Experimental pathology of the liver: Restoration of the liver of the white rat following partial surgical removal. *Arch Pathol.* 1931; 12: 186–202.
38. **Satyanarayana A, Wiemann SU, Buer J, Lauber J, Dittmar KE, Wustefeld T, Blasco MA, Manns MP, Rudolph KL.** Telomere shortening impairs organ regeneration by inhibiting cell cycle re-entry of a subpopulation of cells. *EMBO J.* 2003; 22: 4003–13.
39. **Honkanen RE, Dukelow M, Zwiller J, Moore RE, Khatra BS, Boynton AL.** Cyanobacterial nodularin is a potent inhibitor of type 1 and type 2A protein phosphatases. *Mol Pharmacol.* 1991; 40: 577–83.
40. **Meriluoto JA, Nygard SE, Dahlem AM, Eriksson JE.** Synthesis, organotropism and hepatocellular uptake of two tritium-labeled epimers of dihydromicrocystin-LR, a cyanobacterial peptide toxin analog. *Toxicon.* 1990; 28: 1439–46.
41. **Eriksson JE, Toivola D, Meriluoto JA, Karaki H, Han YG, Hartshorne D.** Hepatocyte deformation induced by cyanobacterial toxins reflects inhibition of protein phosphatases. *Biochem Biophys Res Commun.* 1990; 173: 1347–53.
42. **Yan Y, Mumby MC.** Distinct roles for PP1 and PP2A in phosphorylation of the retinoblastoma protein. PP2a regulates the activities of G(1) cyclin-dependent kinases. *J Biol Chem.* 1999; 274: 31917–24.
43. **Song KY, Lim IK, Park SC, Lee SO, Park HS, Choi YK, Hyun BH.** Effect of nodularin on the expression of glutathione S-transferase placental form and proliferating cell nuclear antigen in N-nitrosodiethylamine initiated hepatocarcinogenesis in the male Fischer 344 rat. *Carcinogenesis.* 1999; 20: 1541–8.
44. **Schulte-Hermann R.** [Feeding rhythms and the diurnal rhythm of cell proliferation in pharmacologically induced liver growth (author's transl)]. *Arch Toxicol.* 1976; 36: 235–45.
45. **Tessitore L, Tomasi C, Greco M.** Fasting-induced apoptosis in rat liver is blocked by cycloheximide. *Eur J Cell Biol.* 1999; 78: 573–9.
46. **Hara E, Smith R, Parry D, Tahara H, Stone S, Peters G.** Regulation of p16CDKN2 expression and its implications for cell immortalization and senescence. *Mol Cell Biol.* 1996; 16: 859–67.
47. **Dimri GP, Lee X, Basile G, Acosta M, Scott G, Roskelley C, Medrano EE, Linskens M, Rubelj I, Pereira-Smith O.** A biomarker that identifies senescent

human cells in culture and in aging skin *in vivo*. *Proc Natl Acad Sci USA.* 1995; 92: 9363–7.

48. **Gorla GR, Malhi H, Gupta S.** Polyploidy associated with oxidative injury attenuates proliferative potential of cells. *J Cell Sci.* 2001; 114: 2943–51.
49. **Sigal SH, Rajvanshi P, Gorla GR, Sokhi RP, Saxena R, Gebhard DR Jr, Reid LM, Gupta S.** Partial hepatectomy-induced polyploidy attenuates hepatocyte replication and activates cell aging events. *Am J Physiol.* 1999; 276: G1260–72.
50. **Nagy P, Teramoto T, Factor VM, Sanchez A, Schnur J, Paku S, Thorgeirsson SS.** Reconstitution of liver mass via cellular hypertrophy in the rat. *Hepatology.* 2001; 33: 339–45.
51. **van Gijssel HE, Maassen CB, Mulder GJ, Meerman JH.** p53 protein expression by hepatocarcinogens in the rat liver and its potential role in mitoinhibition of normal hepatocytes as a mechanism of hepatic tumour promotion. *Carcinogenesis.* 1997; 18: 1027–33.
52. **Laconi S, Pani P, Pillai S, Pasciu D, Sarma DS, Laconi E.** A growth-constrained environment drives tumor progression *in vivo. Proc Natl Acad Sci USA.* 2001; 98: 7806–11.
53. **Jung A, Schrauder M, Oswald U, Knoll C, Sellberg P, Palmqvist R, Niedobitek G, Brabletz T, Kirchner T.** The invasion front of human colorectal adenocarcinomas shows co-localization of nuclear beta-catenin, cyclin D1, and $p16^{INK4a}$ and is a region of low proliferation. *Am J Pathol.* 2001; 159: 1613–7.
54. **Malumbres M, Sotillo R, Santamaria D, Galan J, Cerezo A, Ortega S, Dubus P, Barbacid M.** Mammalian cells cycle without the D-type cyclin-dependent kinases Cdk4 and Cdk6. *Cell.* 2004; 118: 493–504.
55. **Kozar K, Ciemerych MA, Rebel VI, Shigematsu H, Zagozdzon A, Sicinska E, Geng Y, Yu Q, Bhattacharya S, Bronson RT, Akashi K, Sicinski P.** Mouse development and cell proliferation in the absence of D-cyclins. *Cell.* 2004; 118: 477–91.
56. **Geng Y, Yu Q, Sicinska E, Das M, Schneider JE, Bhattacharya S, Rideout WM, Bronson RT, Gardner H, Sicinski P.** Cyclin E ablation in the mouse. *Cell.* 2003; 114: 431–43.
57. **Ortega S, Prieto I, Odajima J, Martin A, Dubus P, Sotillo R, Barbero JL, Malumbres M, Barbacid M.** Cyclin-dependent kinase 2 is essential for meiosis but not for mitotic cell division in mice. *Nat Genet.* 2003; 35: 25–31.
58. **Ramsey MR, Krishnamurthy J, Pei XH, Torrice C, Lin W, Carrasco DR, Ligon KL, Xiong Y, Sharpless NE.** Expression of $p16^{INK4a}$ compensates for p18Ink4c loss in cyclin-dependent kinase 4/6-dependent tumors and tissues. *Cancer Res.* 2007; 67: 4732–41.
59. **Fiorino AS, Diehl AM, Lin HZ, Lemischka IR, Reid LM.** Maturation-dependent gene expression in a conditionally transformed liver progenitor cell line. *In vitro Cell Dev Biol Anim.* 1998; 34: 247–58.
60. **Nagy P, Bisgaard HC, Thorgeirsson SS.** Expression of hepatic transcription factors during liver development and oval cell differentiation. *J Cell Biol.* 1994; 126: 223–33.
61. **Jelnes P, Santoni-Rugiu E, Rasmussen M, Friis SL, Nielsen JH, Tygstrup N, Bisgaard HC.** Remarkable heterogeneity displayed by oval cells in rat and mouse models of stem cell-mediated liver regeneration. *Hepatology.* 2007; 45: 1462–70.
62. **Gossen M, Bujard H.** Tight control of gene expression in mammalian cells by tetracycline-responsive promoters. *Proc Natl Acad Sci USA.* 1992; 89: 5547–51.
63. **Gossen M, Freundlieb S, Bender G, Muller G, Hillen W, Bujard H.** Transcriptional activation by tetracyclines in mammalian cells. *Science.* 1995; 268: 1766–9.